

MRI Techniques for the Examination of Trabecular Bone Structure

M. Petrantonaki, T. Maris and J. Damilakis*

Department of Medical Physics, Faculty of Medicine, University of Crete, P.O. Box 2208, Iraklion 71003, Crete, Greece

Abstract: It is well known that bone mineral density measurement is a widely available means of identifying individuals with osteoporosis. However, bone strength depends not only on the amount of material but also on properties related to bone quality. Significant progress has been made in the development of magnetic resonance imaging (MRI) techniques for assessing bone status during the past years. This review discusses the technical principles, clinical applications, recent advances, limitations, and future trends of MRI techniques available for the diagnosis of osteoporosis. Using MRI, bone status can be evaluated either by T2* measurements, which are sensitive to field inhomogeneities caused by susceptibility differences at the marrowbone interfaces, or by high-resolution imaging. In T2* relaxometry, the decrease in marrow T2* measurements and its decay characteristics provide useful information about the structure and quality of the trabecular bone. T2* measurements have been performed at several locations of the axial and peripheral skeleton such as spine, proximal femur and calcaneus. It has also been shown that osteoporotic and normal subjects may be distinguished using T2* decay characteristics. In addition to T2* relaxometry, high-resolution MR imaging may be used to quantify trabecular bone architecture. Gradient echo and spin echo sequences have been used to obtain images *in vitro* and *in vivo* mainly at peripheral sites of the skeleton. Several image-processing methods have been applied to measure bone structure. Technological advances in MRI scanners offer exciting new possibilities in bone analysis and may contribute to our understanding of osteoporosis.

Keywords: Magnetic resonance imaging, MR relaxometry, high resolution MR, osteoporosis.

INTRODUCTION

Osteoporosis is characterised by loss of bone mineral in the human skeleton due to metabolic changes associated mainly with aging. The disease progressively affects the micro-architectural structure of bone leading to increased bone fragility and, hence, to increased atraumatic fracture risk. Although the skeleton is composed mostly of cortical bone, it is the trabecular bone, with its high metabolic function, that is the primary site for early bone loss. For this reason, several techniques developed for the diagnosis of osteoporosis are confined to the skeletal sites with high trabecular content such as spine, proximal femur, distal forearm and os calcis. Measurements at these locations would reflect the bone loss due to their high metabolic activity.

Bone mineral density (BMD) is the parameter mainly used for the quantification of osteoporosis. However, it is known that BMD is not the sole determinant of the bone strength and that trabecular architecture underlies osteoporotic fractures [1,2]. Specifically, BMD accounts for about 80% of the variance in bone strength [3]. The other 20% could be accounted for by factors related to bone architecture. This may partially explain the overlapping BMD values that were observed between patients with and without osteoporotic fractures [4].

Over the last decades, several techniques have been developed for the assessment of bone status. Dual-energy x-ray absorptiometry (DXA) is currently the most widely used

method for the measurement of BMD. Moreover, quantitative computed tomography has provided images that reflect bone density. However, research focuses to the development of techniques capable of evaluating the micro-architectural characteristics of bone. Magnetic Resonance Imaging (MRI) techniques developed for diagnosis of osteoporosis are promising in this perspective.

A growing literature indicates that MRI may provide information not only on bone density but also on bone structure. Two major approaches have been developed utilizing MR techniques. The first is referred to as indirect MR imaging or relaxometry or quantitative magnetic resonance and is based mainly on the estimation of T2* decay characteristics of bone marrow in the inter-trabecular spaces of cancellous bone [5,6]. The second approach portrays directly the 2D or 3D trabecular bone structure utilizing high spatial resolution MR images [7,8]. The trabecular bone appears as a signal void while bone marrow has uniform high signal intensity, yielding either a direct depiction of trabeculae on a high resolution tomographic image or a binary type post-processed image map. It requires, however, a high field technology for a high spatial resolution and a high signal-to-noise ratio (SNR) to be achieved.

RELAXOMETRY

Standard MRI techniques on conventional medium-to-high field MR systems are used to study the density and quality of trabecular bone structure in various skeletal sites. Bone marrow T2* relaxation time is the parameter more often used as an index of the inhomogeneities in trabecular bone structure and therefore as an index of osteoporosis [9-11]. T1 relaxation time increases as the bone density

*Address correspondence to this author at the University of Crete, Faculty of Medicine, Medical Physics Department, P.O.Box 2208, 71003 Iraklion, Crete, Greece; Tel: +30-2810-392569; Fax: +30-2810-542095; E-mail: damilaki@med.uoc.gr

increases whereas T2 relaxation time values are low in cortical and trabecular bone due to lack of water. However, the presence of bone marrow material in contact to trabecular bone structure causes modifications mainly to relaxation time T2* due to differences in diamagnetic susceptibility between the two [12]. In the presence of a magnetic field, this susceptibility difference at the interface causes additional spatial inhomogeneities to the static field that will be reflected in a decrease of T2* of the bone marrow protons. The change in bone marrow T2* and its decay characteristics provides useful information for the density and structure of the trabecular matrix and its surroundings [13-15]. During aging the trabecular bone density will decrease and structural changes will appear to the bone architecture that will also induce changes of T2* of bone marrow [16,17]. Several techniques are used for direct assessment of T2*, most of them based on gradient echo (GRE) protocols [5,11,18] (Fig. 1). Multiple spin-echo (MSE) techniques more often used for the calculation of the T2 (Fig. 2) are also utilized for the evaluation of trabecular bone quality [19]. In the last few years, however, new sequences have been applied for quantitative MRI [20-22].

***In Vitro* Relaxometry Studies**

Brismar *et al.* used specimens of defatted human lumbar vertebrae to study inhomogeneities caused by susceptibility differences between trabecular bone and surrounding water at 1.5 T field strength [20]. Good correlation between R2' ($R2' = R2^* - R2$) and bone mineral content (BMC), bone mineral per area and BMD was found. R2 ($R2 = 1/T2$) was also positively correlated with the above parameters except from the BMD. T2* appeared shorter in the case of water presence in the trabecular spaces compared with that of pure water at a 0.6 T field strength [15]. Experimental studies in water with and without bone powder at a 5.9 T magnetic field showed also a reduction in the T2* relaxation time of the water in the presence of bone powder [23].

Several *in vitro* studies have also been undertaken for the estimation of correlation factors between R2* and BMD [20, 24]. In a study performed by Majumdar *et al.* T1, T2 and T2* marrow relaxation times were measured using a 1.5 T magnet in specimens of vertebral bodies. The measurements were correlated with BMD values [16]. The orientation of the trabecular bone in the magnetic field has been found to be important for T2* variations [25]. Phantom studies have also been conducted to investigate the impact of trabecular structure on MR relaxation times [26,27]. The results demonstrate that the MR signal is affected not only by density but also by trabecular microstructure.

***In Vivo* Relaxometry**

Several *in vivo* studies showed that T2* relaxation time increases with loss of bone density and thus with age [10,28]. Funke *et al.* obtained in the lumbar spine an average T2* of 13.4 ms for normal subjects compared with 19.9 ms for osteoporotic patients [28]. Link *et al.* measured T2* of the proximal femur to be about 18-19 ms in postmenopausal normal subjects and 21-23 ms in postmenopausal patients with osteoporosis [29]. Bone marrow T2* also decreases in the presence of trabecular bone in GRE [13]. The loss of signal depends on the region of measurement and is found to

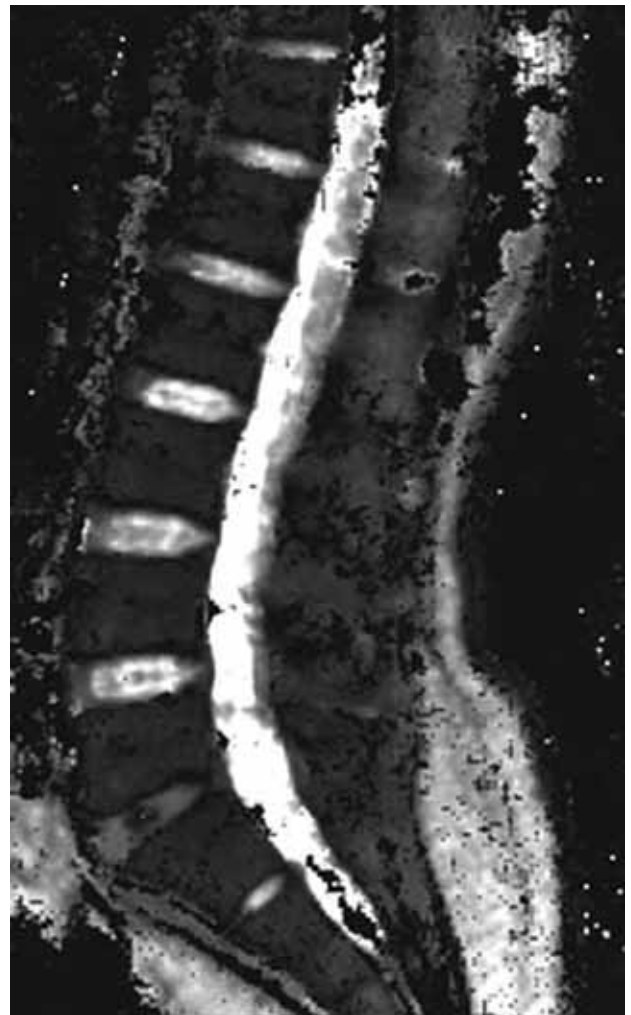


Fig. (1). T2* calculated image map obtained from a middle sagittal slice through the lumbar spine of a non-osteoporotic postmenopausal subject. A 2D multi echo gradient Echo (GRE) sequence with 32 repeatable equidistant gradient echoes (TE's: 2.7-74.3 ms) was used for the calculation of T2* on a pixel by pixel basis. The pixel in plane resolution is 0.7 mm X 0.7 mm and cross plane resolution (slice thickness) is 10 mm. An average T2* of 13 ± 2 ms was measured for the first four lumbar vertebrae.

be higher in the epiphysis and less in the diaphysis [30]. This effect is more pronounced in the T2* rather than the T2 measurements (Fig. 3a,b).

Positive correlations between T2', T2* and BMD were observed in several *in vivo* studies at different skeletal sites such as the calcaneus [31,32], distal radius [18] and femoral neck [29,31]. However, Link *et al.* showed that stronger correlation exists between T2* and age in proximal femur as compared to the correlation of BMD and age [29]. Fransson *et al.* showed moderate to strong correlations between BMD in the proximal femur and T2* in tibia, while ultrasound parameters measured on the calcaneus demonstrated significantly weaker correlations to the MR parameters. The latter has been explained to be due to single-point ultrasound assessment as well as due to the heterogeneity of bone matrix in the tibia [33]. Several studies have shown that MRI

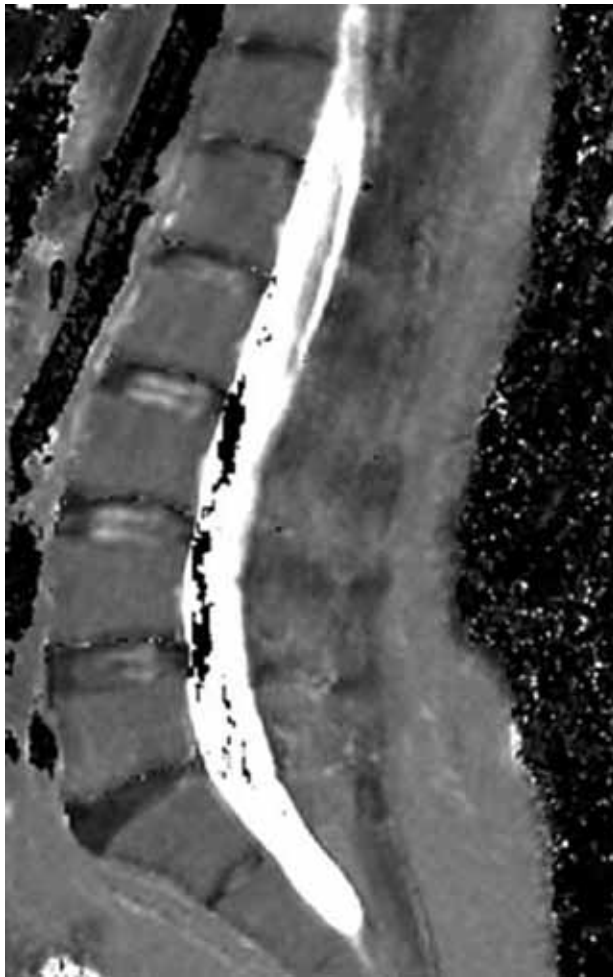


Fig. (2). T2 calculated image map obtained from a middle sagittal slice through the lumbar spine of a non osteoporotic postmenopausal subject. A 2D multi echo Spin Echo (SE) sequence with 16 repeatable equidistant spin echoes (TE's: 22.5-360 ms) was used for the calculation of T2 on a pixel by pixel basis. The pixel in plane resolution is 0.7 mm X 0.7 mm and cross plane resolution (slice thickness) is 10 mm. An average T2 of 78 ± 5 ms was measured for the first four lumbar vertebrae.

measurements may be affected by density and structure variations at different sites of the heel [34-37]. Song *et al.* showed large regional variations within the calcaneus and a dependence of $R2'$ on the angle of the foot relative to the direction of the static magnetic field [37]. Therefore, it would be useful to determine the most appropriate site on the calcaneus at which reproducible and reliable MR measurements can be made.

Limited studies have been published regarding MR relaxometry of the lumbar spine [11,31]. Lumbar spine T2 measurements (Fig. 2) show strong correlation with BMD whereas lumbar spine T2* (Fig. 1) and T2' relaxation times are more sensitive in assessing lumbar spine osteoporosis [22]. Bone marrow T2* at the radius and spine has also demonstrated a good correlation with BMD. This is accompanied with an age-related decrease of R2* at both sites [11,38]. Wehrli *et al.* showed that the ability to discriminate between patients with and without vertebral

osteoporotic fractures is improved when relaxation times and BMD are combined [39].

HIGH RESOLUTION (HR) MRI

Several imaging methods have been used to analyse the trabecular bone structure such as conventional and projectional radiograph, HR MRI and HR computed tomography. MRI appears to be ideal due to the lack of ionizing radiation and the additional information it offers concerning bone quality.

HR MRI has been used to obtain images of the trabecular bone structure in the peripheral skeleton. Recent software and hardware advances such as high-field scanners, fast and powerful gradients and new coil designs provide trabecular bone images with spatial resolution of 80-150 microns in plane and slice thickness as low as 300 μ m *in vivo* and *in vitro*. Modified 3D GRE and SE sequences may be used to obtain these images. Majumdar *et al.* evaluated the relative importance of TE in GRE MR imaging [40]. They found that the structural parameters depend on the echo time used to obtain the MR images. TE is mainly affected by the receiver bandwidth used to sample the MR signal. The higher the bandwidth used to sample the MR signal, the shorter is the applied TE. However, with a higher bandwidth the SNR is reduced. To increase SNR in the image, either the repetition time TR or the number of signal excitations (signal averaging) may be increased which in turn will negatively affect the overall MRI examination time [41]. Thus, factors such as TE, receiver bandwidth and number of signal excitations may significantly affect MR image quality.

The main structural parameters measured are the apparent trabecular thickness (Tb. Th), trabecular bone volume fraction (BV/TV), trabecular spacing (Tb. Sp) and trabecular number (Tb. N.) [42,43]. These parameters originate from bone histomorphometry and are measured in 2D cross section images (partitions) of the three dimensional trabecular bone sections. Various image processing and analysis algorithms have been developed for the above quantitative estimation of parameters ranging from ROI's determination, filtering, reversed grey scale to segmentation into bone (white pixels) and marrow (black pixels) and length analysis methods [44-46]. Texture and morphology related parameters, such as 'fractal dimension', and 'complexity of the network' calculated via a standard box-counting algorithm technique [47], might also be used to characterize the trabecular bone structure and pattern from MR images [48].

In Vitro HR- MR Studies

In vitro trabecular bone structure assessment at a high spatial resolution of 92 μ m showed good correlation between parameters obtained by 3D MR reconstruction images and those determined by 2D optical images: for BV/TV $R^2 = 0.81$, for Tb. N $R^2 = 0.53$ and for Tb. Sp $R^2 = 0.73$ [49]. At lower spatial resolution (156x156x300 μ m³) partial volume effects result in an underestimation of Tb.Sp (approximately 1.6 times) and Tb. N together with an overestimation of BV/TV and Tb. Th (approximately 3 times) [46]. The variation of structural parameters was also examined by Kothari *et al.* using 3D optical reconstruction of trabecular bone specimens [50]. Image resolution was varied from

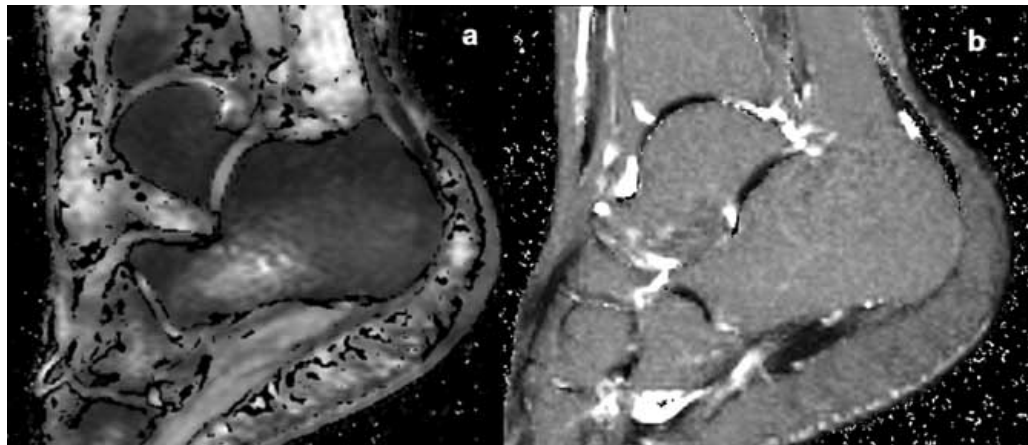


Fig. (3). T2* calculated (a) and T2 calculated (b) image maps obtained from a sagittal slice through the calcaneus of a non osteoporotic postmenopausal subject. A 2D multi echo gradient Echo (GRE) sequence with 32 repeatable equidistant gradient echoes (TE's: 2.7-74.3 ms) was used for the calculation of T2* (a) and a 2D multi echo spin echo (SE) sequence with 16 repeatable equidistant spin echoes (TE's: 22.5-360 ms) was used for the calculation of T2 (b) on a pixel by pixel basis. The pixel in plane resolution is 0.5 mm X 0.5 mm and cross plane resolution (slice thickness) is 10 mm. An average T2* of 18 ± 3 ms and average T2 of 102 ± 6 ms were measured for the whole calcaneal area. Note the loss of signal (shorter T2*) in the epiphysial regions of the calcaneus present on the T2* images (a) which is clearly not present on the T2 images (b).

$40 \times 40 \times 40 \mu\text{m}^3$ to $100 \times 100 \times 1000 \mu\text{m}^3$. Tb. Th showed rapid increase at higher slice thickness in contrast with the other parameters that indicated a weaker dependency. The effect of slice thickness on standard morphologic measurements on calcaneus specimens was estimated by Vieth *et al.* using HR MRI with slice thickness of $300 \mu\text{m}$ to $900 \mu\text{m}$ and contact radiographs. Significant correlations between parameters were observed, especially for BV/TV and Tb. Th. Partial volume effects were less pronounced at small slice thickness [51].

A comparison between MR based measures and BMD values on trabecular bone specimens showed that as BMD increases all three but the Tr. Sp are also increased [41]. A MR-based structural study on specimens of several skeletal sites with varying density in conjunction with BMD measurements was conducted by Majumdar *et al.* [52]. The biomechanical elastic modulus was also measured along the three orthogonal axes and correlated with the structural parameters. The assessment of trabecular bone 3D-architectural properties improves the assessment of the biochemical trabecular bone characteristics. Antich *et al.* used MRI to diagnose changes in trabecular bone structure after fluoride therapy [53].

In Vivo HR- MR Imaging

The accuracy of the *in vivo* HR MR imaging techniques in the assessment of osteoporosis depends mostly on several MR related technical factors such as magnetic field strength, coil type, gradient strength and speed (slew rate) as well as sequence type and parameter selection. Spin-echo (SE) sequences are less sensitive to susceptibility artifacts present at the bone-bone marrow interfaces and they are preferred for bone structure quantification measurements [40]. However, acquisitions times as long as 20 minutes or more are often required for the completion of a single MR imaging protocol. GRE based sequences although sensitive to susceptibility artifacts are faster than SE sequences by a

factor of two. Compensation for the susceptibility artifacts can be achieved by the choice of adequate sequence parameters and appropriate shimming prior to imaging.

Generally, the spatial resolution obtained in clinical scanners in *in-vivo* studies is limited by the low SNR of the images. Faster gradients (shorter TE's) and dedicated surface coils achieve higher SNR's. However, the maximum achievable accuracy and efficacy is required for the quantitative analysis of a structure on a HR MR image. Several image post-processing techniques applied on HR MR images were developed concerning this task. These include : (a) histogram deconvolution to obviate binary segmentation [54], (b) morphological filter techniques [55], (c) autocorrelation functions and co-occurrence matrices [56], (d) receiver operating characteristic analysis [57], (e) distance transformation methods [58], (f) digital topological analysis [59] and (g) finite element analysis [60]. In an effort for further software development, an automatic system for the characterization of trabecular bone structure utilizing HR MR images has been developed by Newitt *et al.* [61]. The reproducibility of the system performance is found to be depended on the image quality and is estimated to be of 2-4% for 2D structural parameters and 4-9% for 3D mechanical parameters.

Recently, an advanced texture analysis tool was introduced by Langenberger *et al.* [62]. In this study, the bone homogeneity factor (BHF) was introduced as an index for the quantitative measurement of bone structure. BHF is measured on HR MR images of the calcaneus. Correlations of BHF with DXA measurements of the femoral neck were found to be significant ($r = 0.73$). The authors concluded that BHF is a potential index of skeletal status possible and could possibly be used to distinguish osteoporotic and non osteoporotic bone.

The necessity of artifact free, higher spatial resolution, higher SNR images, leads the investigators to focus rather on MR studies of the peripheral skeleton than that of the spine. Numerous *in vivo* studies were performed in the distal radius where osteoporotic fractures are commonly present. The calcaneus (Fig. 4a,b) is another preferable skeletal position and is often used for the prediction of fractures for other skeletal sites. Both sites of peripheral skeleton are easily adapted to the HR MR imaging techniques. Recent studies also show interest in the use of HR MRI for the visualization of the bone microstructure in the finger phalanges [63, 64].

Majumdar *et al.* obtained HR MR images of the distal radius in premenopausal normal, postmenopausal normal and postmenopausal osteoporotic women [8]. The parameters calculated were apparent measures of BV/TV, Tb. Th, Tb. Sp and Tb. N and fractal based morphological parameters such as the 'box-counting dimension'. The associations between the indices of trabecular bone structure measured by HR MR images and either BMD or BMC in the distal radius were examined. Cortical BMC and trabecular BMD of the distal radius as well as BV/TV, Tb. Th and Tb. N were decreased with age. Tb. Sp and Tb. N showed moderate correlation with radial trabecular BMD and poor correlation with radial cortical BMC.

Link *et al.* used HR MR images of the calcaneus to investigate the differences between the trabecular structure of patients with and without osteoporotic hip fractures [34]. A 3D GRE sequence was used with slice thickness of 500 μm and in plane resolution of 195 μm^2 . Texture analysis was performed to assess morphological parameters and fractal dimension. MRI measurements were found superior to proximal femur BMD estimations. In addition, all trabecular structure measurements derived from MR other than Tb.Th were found to be able to differentiate between postmenopausal women with and without osteoporotic hip fractures ($p < 0.05$).

In a similar study, Majumdar *et al.* analysed HR MR images of trabecular bone in the distal radius and compared their findings with (a) HR images of the calcaneus (b) BMD at the hip and (c) BMD at the distal radius for the prediction of prevalent hip fractures [43]. Measurements of apparent Tb. Sp and apparent Tb. N in the distal radius and hip BMD estimations showed significant differences ($p < 0.05$) when compared between patients with hip fractures and normal age-matched postmenopausal subjects. This was not observed in radial BMD measurements ($p = 0.05$).

Wehrli *et al.* analysed MR microimages of the radius obtained from women of varying BMD and spinal deformity status [59]. The images were analysed and the parameters derived were compared with the integral BMD of the lumbar spine and femur as well as with the MR derived BV/TV. Structural indices were found to discriminate between patients with and those without deformities in the spine. Moreover, measures of the ratio of platelike to rodlike trabeculae, which are the surface-to-curve ratio and topological surface density, were found to be lower in subjects with spinal deformities. Their study provide the first *in vivo* evidence of the structural changes appearing in postmenopausal osteoporotic women due to the conversion of trabecular plates to rods and the further disruption of rods due to repeated osteoclastic resorption.

Link *et al.* analysed the trabecular bone structure of the calcaneus utilising HR MRI in male patients before and after cardiac transplantation and compared their results with BMD measurements [65]. The aim of their study was to predict therapy-induced bone loss and vertebral spine fracture status. Vertebral fractures were found in 36% of the post-cardiac transplantation patients. According to their results, MRI of the calcaneus can be used to diagnose changes in the trabecular bone structure following cardiac transplantation. A similar study was also performed by Link *et al.* in patients before and after renal transplantation [57]. Using receiver

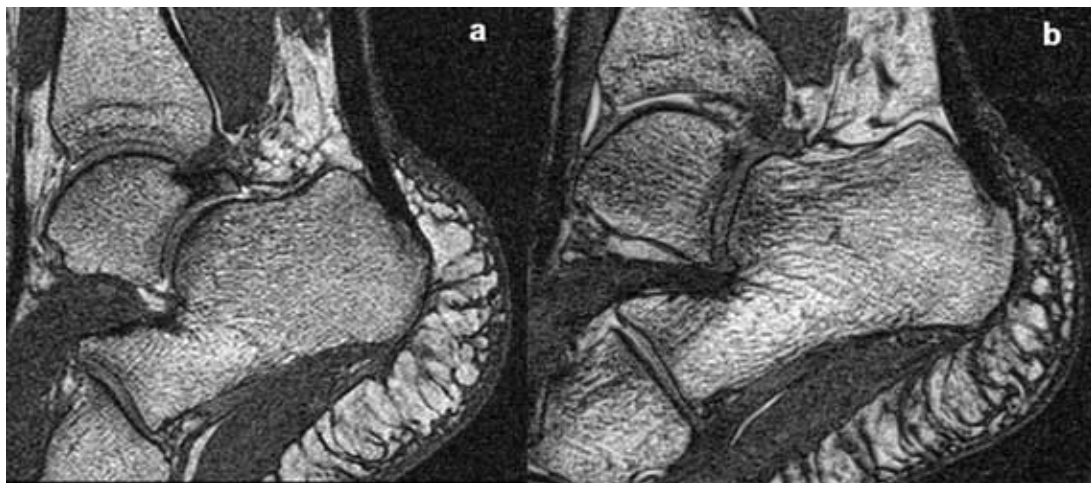


Fig. (4). *In vivo* high resolution MR images obtained using a 3D Double Echo Steady State (DESS) sequence depicting a sagittal plane for a non osteoporotic (a) and an osteoporotic (b) postmenopausal subject. The pixel in plane resolution is 200 μm X 200 μm and cross plane resolution (slice thickness) is 100 μm . A 10 mm sagittal slab with 10 partitions (1 mm slice thickness) is obtained in a total acquisition time of 4 mins. Note the heterogeneity in the trabecular bone structure, with marked anisotropy in the subtalar region as compared with the more uniform posterior region. These effects are more pronounced in the osteoporotic (b) rather than the non osteoporotic (a) subject.

operating characteristic analysis, the highest diagnostic performance was found when using a combination of BMD status and structural measurements derived from HR images of the calcaneus.

CONCLUSIONS

Over the last decade research into the role of MR has shown its potential to be a useful method for evaluating bone density and bone micro-structural information. Deep analysis of trabecular bone density and architecture using MRI and its relationship to bone biomechanics is an exciting field for the early diagnosis of osteoporosis. *In vitro* studies have found good correlations between MR derived parameters and histomorphometric measurements. It has also been shown that osteoporotic and non-osteoporotic fractures may be distinguished *in vivo*, following the advent of recent MRI technology and using processing software tools. However, future improvements in MR technology (new coil designs, parallel imaging techniques, gradient performance) and advanced image post-processing software tools are of vital importance in order to realise the real potential of non-invasive, non ionising MR techniques for the accurate assessment of osteoporosis

REFERENCES

- [1] Kleerkoper M, Villanueva AR, Stanciu J, Sudhaker Rao D, Parfitt AM. The role of three-dimensional trabecular microstructure in the pathogenesis of vertebral compression fractures. *Calcif Tissue Int* 1985; 37: 594-597.
- [2] Goldstein SA, Goulet R, McCubbrey D. Measurements and significance of three-dimensional architecture to the mechanical integrity of trabecular bone. *Calcif Tissue Int* 1993; 53 (Suppl 1): S127-S133.
- [3] McCalden RW, McGeough JA, Barker MB, Court-Brown CM. Age-related changes in porosity, mineralization and microstructure. *J Bone Joint Surg Am* 1993; 75: 1193-1205.
- [4] Link TM. In: Link TM Ed, *Radiology of osteoporosis*. Berlin, Springer-Verlag 2003; 143-164.
- [5] Davis CA, Genant HK, Dunham JS. The effects of bone on proton NMR relaxation times of surrounding liquids. *Invest Radiol* 1986; 21: 472-477.
- [6] Rosenthal H, Thulborn KR, Rosenthal DI, Rosen BR. Magnetic susceptibility effects of trabecular bone on magnetic resonance bone marrow imaging. *Invest Radiol* 1990; 25: 173-178.
- [7] Hwang SN, Wehrli FW, Williams JL. Probability-based structural parameters from three-dimensional nuclear magnetic resonance images as predictors of trabecular bone strength. *Med Phys* 1997; 24: 1255-1261.
- [8] Majumdar S, Genant HK, Grampp S, Newitt DC, Truong VH, Lin JC, Mathur A. Correlation of trabecular bone structure with age, bone mineral density, and osteoporotic status: *In vivo* studies in the distal radius using high resolution magnetic resonance imaging. *J Bone Miner Res* 1997; 12: 111-118.
- [9] Ford J, Wehrli F, Chung H. Magnetic field distribution in models of trabecular bone. *Magn Reson Med* 1993; 17: 543-551.
- [10] Wehrli FW, Ford JC, Attie M, Kressel H, Kaplan F. Trabecular structure : preliminary application of MR interferometry. *Radiology* 1991; 179: 615-621.
- [11] Wehrli FW, Ford JC, Haddad GJ. Osteoporosis: Clinical assessment with quantitative MR imaging in diagnosis. *Radiology* 1995; 196: 631-641.
- [12] Hopkins JA, Wehrli FW. Magnetic susceptibility measurement of insoluble solids by NMR: Magnetic susceptibility of bone. *Magn Reson Med* 1997; 37: 494-500.
- [13] Sebag GH, Moore SG. Effects of trabecular bone on the appearance of marrow in gradient echo imaging of the appendicular skeleton. *Radiology* 1990; 174: 855-859.
- [14] Majumdar S, Genant H. *In vivo* relationship between marrow T2* and trabecular bone density determined with a chemical shift-selective asymmetric spin-echo sequence. *Magn Reson Imaging* 1992; 2: 209-219.
- [15] Ford J, Wehrli F. *In vivo* quantitative characterization of trabecular bone by NMR interferometry and localized proton spectroscopy. *Magn Reson Med* 1991; 17: 543-551.
- [16] Majumdar S. Quantitative study of the susceptibility difference between trabecular bone and bone marrow: Computer simulations. *Magn Reson Med* 1991; 22: 101-110.
- [17] Majumdar S, Thomasson D, Shimakawa A, Genant HK. Quantitation of the susceptibility difference between trabecular bone and bone marrow: Experimental studies. *Magn Reson Med* 1991; 22: 111-127.
- [18] Grampp S, Majumdar S, Jergas M, Lang P, Gies A, Genant HK. MRI of bone marrow in the distal radius: *in vivo* precision of effective transverse relaxation times *Eur Radiol* 1995; 5: 43-8.
- [19] Capuani S, Alessandri FM, Bifone A, Maraviglia B. Multiple spin echoes for the evaluation of trabecular bone quality. *MAGMA* 2002; 14: 3-9.
- [20] Brismar TB, Karlsson M, Li TQ, Ringertz H. The correlation between R2' and bone mineral measurements in human vertebrae: an *in vitro* study. *Eur Radiol* 1999; 9: 141-144.
- [21] Ma J, Wehrli FW. Method for image-based measurement of the reversible and irreversible contribution to the transverse relaxation rate. *J Magn Reson Ser B*, 1996; 111: 61-69.
- [22] Maris TG, Damilakis J, Sideri L, *et al.* Assessment of the skeletal status by MR relaxometry techniques of the lumbar spine: comparison with dual X-ray absorptiometry. *Eur J Radiol* 2004; 50: 245-56.
- [23] Davis JW, Grove JS, Ross PD, Vogel JM, Wasnich RD. Relationship between bone mass and rates of bone change at appendicular measurement sites. *J Bone Miner Res* 1992; 7: 719-725.
- [24] Kang C, Paley M, Ordidge R, *et al.* R2' measured in trabecular bone *in vitro*: Relationship to trabecular separation. *Magn Reson Imaging* 1999; 17: 989-995.
- [25] Takahashi M, Wehrli FW, Hwang SN, *et al.* Relationship between cancellous bone induced magnetic field and ultrastructure in a rat ovariectomy model. *Magn Reson Imaging* 2000; 18: 33-39.
- [26] Engelke K, Majumdar S, Genant HK. Phantom studies simulating the impact of trabecular structure on marrow relaxation time, T2'. *Magn Reson Med* 1994; 31: 384-387.
- [27] Selby K, Majumdar S, Newitt DC, *et al.* Investigation of MR decay rates in microphantom models of trabecular bone. *J Magn Reson Imaging* 1996; 6: 549-559.
- [28] Funke M, Bruhn H, Vosschenrich R, Rudolph O, Grabbe E. Bestimmung der T2*- Relaxationszeit zur Charakterisierung des trabekulären Knochens. *Fortschr Roentgenstr* 1994; 161: 58-63.
- [29] Link TM, Majumdar S, Augat P, *et al.* Proximal femur: Assessment of osteoporosis with T2* decay characteristics at MR imaging. *Radiology* 1998; 209: 531-536.
- [30] Ford JC, Wehrli FW. *In vivo* quantitative characterization of trabecular bone by NMR interferometry and localized proton spectroscopy. *Magn Reson Med* 1991; 17: 543-551.
- [31] Brismar TB. MR relaxometry of lumbar spine, hip and calcaneus in healthy premenopausal women: relationship with dual energy X-ray absorptiometry and quantitative ultrasound. *Eur Radiol* 2000; 10: 1215-1221.
- [32] Kang C, Paley M, Ordidge R, Speller R. *In vivo* MRI measurements of bone quality in the calcaneus: a comparison with DXA and ultrasound. *Osteoporosis Int* 1999; 9: 65-74.
- [33] Fransson A, Grampp S, Imhof H. Effects of trabecular bone on marrow relaxation in the tibia. *Magn Reson Imaging* 1999; 17: 69-82.
- [34] Link TM, Majumdar S, Augat P, *et al.* *In vivo* high resolution MRI of the calcaneus: Differences in trabecular structure in osteoporosis patients. *J Bone Miner Res* 1998; 1175-1182.
- [35] Guglielmi G, Selby K, Blunt BA, *et al.* Magnetic resonance imaging of the calcaneus: Preliminary assessment of trabecular bone -dependent regional variations in marrow relaxation time compared with dual x-ray absorptiometry. *Acad Radiol* 1996; 3: 336-343.
- [36] Yablonskiy DA, Haacke EM. Theory of NMR signal behavior in magnetically inhomogeneous tissues: The static dephasing regime. *Magn Reson Med* 1994; 32: 749-763.

- [37] Song HK, Wehrli FW, Ma J. Field strength and angle dependence of trabecular bone marrow transverse relaxation in the calcaneus. *J Mag Reson Imag* 1997; 7: 382-388.
- [38] Grampp S, Majumdar S, Jergas M, Newitt D, Lang P, Genant HK. Distal radius: *In vivo* assessment with quantitative MR imaging, peripheral quantitative CT and dual X-ray absorptiometry. *Radiology* 1996; 198: 213-218.
- [39] Wehrli FW, Hopkins JA, Hwang SN, Song HK, Snyder PJ, Haddad JC. Cross-sectional study of osteopenia with quantitative MR imaging and bone densitometry. *Radiology* 2000; 217: 527-538.
- [40] Majumdar S, Newitt D, Jergas M, *et al.* Evaluation of technical factors affecting the quantification of trabecular bone structure using magnetic resonance imaging. *Bone* 1995; 17: 417-430.
- [41] Majumdar S, Genant HK. In: Genant HK, Guglielmi G, Jergas M. Ed., *Bone densitometry and osteoporosis*. Berlin, Springer-Verlag 1998; 407-16.
- [42] Whitehouse WJ. The quantitative morphology of anisotropic trabecular bone. *J Microsc* 1974; 101: 153-168.
- [43] Majumdar S, Link TM, Augat P, *et al.* Trabecular bone architecture in the distal radius using magnetic resonance imaging in subjects with fractures of the proximal femur. *Osteoporos Int* 1999; 10: 231-239.
- [44] Goulet RW, Goldstein SA, Ciarelli MJ, *et al.* The relationship between the structural and orthogonal compressive properties of trabecular bone. *J Biomech* 1994; 27: 375-389.
- [45] Quyang X, Selby K, Lang P, *et al.* High resolution MR imaging of the calcaneus: age-related changes in trabecular structure and comparison with DXA measurements. *Calcif Tissue Int* 1997; 60: 139-47.
- [46] Majumdar S, Newitt DC, Mathur A, *et al.* Magnetic resonance imaging of trabecular bone structure in the distal radius: relationship with X-ray tomographic microscopy and biomechanics. *Osteoporosis Int* 1996; 6: 376-385.
- [47] Meier N, Brinkhaus HA, Brickman P, Peters PE. Digital bone structure analysis, In SCAR 1994, Symposia Foundation, Carlsbad, 1994; 670-675.
- [48] Chung HW, Chu C, Underweiser M, Wehrli F. On the fractal nature of trabecular structure. *Med Phys* 1994; 21: 1535-1549.
- [49] Hipp JA, Jansujwicz A, Simmons CA, *et al.* Trabecular bone morphology using micro-magnetic resonance imaging. *J Bone Miner Res* 1996; 11: 286-297.
- [50] Kothari M, Chen T, Lin J, *et al.* 3-D bone architecture assessment: Impact of image resolution. *Osteoporosis Int* 1997; 7: 289.
- [51] Vieth V, Link TM, Lotter A, *et al.* Does the trabecular bone structure depicted by high-resolution MRI of the calcaneus reflect the true bone structure? *Invest Radiol* 2001; 36: 210-217.
- [52] Majumdar S, Kothari M, Augat P, *et al.* High-resolution magnetic resonance imaging: Three-dimensional trabecular bone architecture and biomechanical properties. *Bone* 1998; 22: 445-454.
- [53] Antich PP, Mason RP, McColl R, Zerwech J, Pak CYC. Trabecular architecture studies by 3D MRI microscopy in bone biopsies. *J Bone Miner Res* 1994; 9S1: 327.
- [54] Wehrli FW, Hwang SN, Ma J, *et al.* Cancellous bone volume and structure in the forearm: noninvasive assessment with MR microimaging and image processing. *Radiology* 1998; 206: 347-357.
- [55] Majumdar S, Genant HK, Grampp S, *et al.* Analysis of trabecular bone structure in the distal radius using high resolution MRI. *Eur Radiol* 1994; 4: 517-524.
- [56] Link TM, Majumdar S, Grampp S, *et al.* Imaging of trabecular bone structure in osteoporosis. *Eur Radiol* 1999; 9: 1781-1788.
- [57] Link TM, Saborowski, Kisters K, *et al.* Changes in calcaneal trabecular bone structure assessed with high-resolution MR imaging in patients with kidney transplantation. *Osteoporos Int* 2002; 13: 119-129.
- [58] Laib A, Newitt DC, Lu Y, Majumdar S. New model measures of trabecular bone structure applied to *in vivo* high-resolution MR images. *Osteoporos Int* 2002; 13: 130-136.
- [59] Wehrli FW, Gomberg BR, Saha PK, *et al.* Digital topological analysis of *in vivo* magnetic resonance microimages of trabecular bone reveals structural implications of osteoporosis. *J Bone Miner Res* 2001; 16: 1520-1531.
- [60] VanRierbergen B, Odgaard A, Kabel J, *et al.* Direct mechanics assessment of elastic symmetries and properties of trabecular bone architecture. *J Biomech* 1996; 29: 1653-1657.
- [61] Newitt DC, van Rietbergen B, Majumdar S. Processing and analysis of *in vivo* high-resolution MR images of trabecular bone for longitudinal studies: reproducibility of structural measures and micro-finite element analysis derived mechanical properties. *Osteoporos Int* 2002; 13: 278-287.
- [62] Langenberger H, Shimizu Y, Windischberger C, *et al.* Bone homogeneity factor: an advanced tool for the assessment of osteoporotic bone structure in high-resolution magnetic resonance images. *Invest Radiol* 2003; 38: 467-472.
- [63] Stampa B, Kuhn B, Liess C, Heller M, Gluer CC. Characterization of the integrity of three-dimensional trabecular bone microstructure by connectivity and shape analysis using high-resolution magnetic resonance imaging *in vivo*. *Top Magn Reson Imaging* 2002; 13: 357-363.
- [64] Kuehn B, Stampa B, Heller M, *et al.* *In vivo* assessment of trabecular bone structure of the human phalanges using high resolution magnetic resonance imaging. *Osteoporosis Int* 1997; 7: 291.
- [65] Link T, Lotter A, Beyer F, *et al.* Post-cardiac transplantation changes in calcaneal trabecular bone structure: a magnetic resonance imaging study. *Radiology* 2000; 217: 855-862.